Journal of Research in Environmental and Earth Sciences, 07 (2019) 186-197
Print ISSN: 2356-5799
Online ISSN: 2356-5802

www.knowledgejournals.com

Research article

Pore-lining and grain-coating chlorites in siliciclastic reservoir sandstones (Acacus formation, Ghadamis basin, Libya), nature and implications for their origin

Eman AB Moh Taktek [a,*], Narjes M Omar Shebli [a]
[a] *Waha Oil Company, Tripoli, Libya.*
** Corresponding author. Tel.: +218 927181159. E-mail address: eman_tek2012@yahoo.com or taktektaktek85@gmail.com (Eman AB. Moh Taktek)*

Article history:
Received 15 March 2019; Received in revised form 14 July 2019.
Accepted 21 August 2019; Available online 2 September 2019.

Abstract
The Acacus formation is found in western Libya in the Murzuq and Ghadamis basins. It outcrops in the southwest on the margins of the Murzuq Basin and continues northward in sub crop into the Ghadamis basin. The formation thins towards, and is then absent over, the Qargaf Arch which separates the two basins. These relationships reflect the tectonic history of the region and the development of the major Paleozoic and Mesozoic sedimentary basins which dominate the structural and stratigraphical framework of Libya.
Evaluation of core samples and composite well logs shows that the Acacus Formation in the Ghadamis Basin can be subdivided into three members. The lower and upper members are sand dominated whereas the middle member is mud dominated.
Textural and compositional analysis of the sands and muds of the studied formation demonstrate that they are commonly very iron-rich. The framework silicate grains are dominantly with quart, feldspar including k-feldspar. Muscovite is an important component in some sandstone levels forming thin mica-rich laminae. Glauconite and detrital chamosite occur as replacement of mica and faecal pellets. Chamosite is also present as the cortex of ooids which have been transported into the sands from an adjacent ooid "factory'. These have been classed as inherited grains. Detrital siderite is also present. Phosphate fragments of teeth, bone and scale tend to occur at the top of the iron-rich layers although apatite is also present as rare grain-coating.
Chlorite has been found in the formation with the four lithofacies. They fall into three categories: uncoated grains; coated grains or ooids and mica replacement grains. Features of these grains, suggests that the final event in their history was as detrital particles although the genesis of the chlorite component was authigenic.

Key words: Mineralogy, Sandstone, Diagenetic features, Chronological relationships, Ghadamis, Libya.

1. Introduction

The Ghadamis Basin was a major site of frontier exploratory activity during the late 1950s, 1960s, and 1970s and the first significant oil in Libya was produced from Devonian sandstones reservoirs in this region. Interest in the area, however, diminished rapidly with discovery of the prolific giant oil fields in late Mesozoic and Tertiary deposits of the Sirte Basin which lies to the east in the north-central part of Libya. Production from this basin has underpinned the Libyan economy for the last thirty years. However, in recent years levelling off of significant finds in the Sirte Basin has seen a necessary renewed exploratory interest in the western province to discover new resources and maintain oil production as the country's economic basis. This second exploration phase began during the mid-late 1980s (Figure 1) with the effort focused mainly on already known Devonian (Tahara, Aouinet, Tadrart) and the Ordovician (Memouniat) reservoirs. More recently it has become clear that the Acacus Formation contains both source and reservoir rocks and oil and gas shows are common. Geochemical analyses have demonstrated that some of the Acacus and Silurian Tannezuft Shale's (which both underlie and are laterally equivalent to the sandstones) are good source rocks (Bishop, 1975). At least two major fields are capable of production from these sandstones at present and many others wells with commercially significant flows of oil have been tested in recent years. Acacus-Tannezuft reservoirs were tested in the C.P.T.L concessions 23 and 61, and concession 70 (northern flank of Ghadamis Basin), where the Acacus proved to be oil bearing. During the last year, in AGOCO concessions NC7 and NC5, the Acacus-Tannezuft reservoirs produced a large amount of hydrocarbons. In the northwestern part of the Ghadamis, in BOCO

concession NC100 the Acacus reservoir showed good petroleum results from 14 wells drilled in the area from nine structures that are oil bearing. These recent exploratory works carried out in widely different parts of the Ghadamis Basin appear to confirm the regional potentiality of the Acacus-Tannezuft Formations as a major petroleum source and they are thus being increasingly targeted.

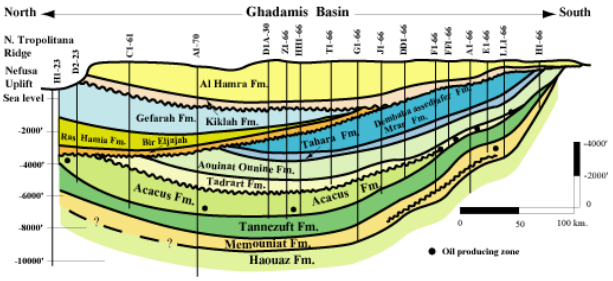

Fig. 1. North-south cross-section showing Acacus Formation distribution along the Ghadamis Basin, where the Acacus proved to be oil bearing, modified from Shah et al. (1993).

The aims of this study is to evaluate the mineralogical composition of the sandstones and mudstones that make up the formation. Objectives include identification of the different detrital and diagenetic minerals, determination of their compositions, their intergranular and intercrystalline relationships and their relative abundances.

2. Materials and methods

2.1. Geographical location of the study area

The Ghadamis Basin is one of a number of major sedimentary basins in Libya a country that occupies the north central region of Africa between Egypt and the Sudan to the east, Tunisia and Algeria to the west, with Niger and Chad situated directly to the south.

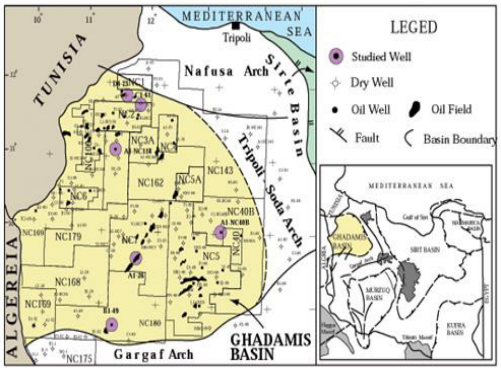

Fig. 2. Geographical location map of Ghadamis Basin, western Libya. Modified from Clifford (1986).

The country covers about 1,800,00 square kilometers and extends about 1925 kilometers from east to west and 1,450 kilometers from north to south. Except for the northernmost parts, which have a Mediterranean climate, the country is substantially Saharan in aspect.

The site of the Ghadamis Basin is located in the western part of the country bordering directly on Algeria and southern Tunisia (Figure 2). The area involved covers a total surface area of 200,000 sq. km.

2.2. Methodology

Ninety-six samples from the recorded sections were chosen for XRD and SEM analyses. They were selected from four major lithofacies; clean sandstone; bioturbated sandstone; iron-rich sandstone, and mudstone.

The nature, morphology, crystallinity and composition of the chlorite mineral observed in the sandstones and mudstones have been investigated using a variety of analytical methods. The morphological descriptions are mostly based on observations made with the SEM. Qualitative and quantitative data on their crystallinity and structure have been obtained using X-ray diffraction (XRD) on the less than 2mm -size fraction. Their elemental compositions have been quantified with the SEM. The clays were initially identified in thin section (Deer et al., 1992), and from X-ray diffractograms by reference to Brown and Brindley (1980). Clay mineral types were further confirmed by DTA analysis.

3. Results and discussion

3.1. Diagenetic sequence in the Acacus formation

Diagenetic features relationships which form the basis of the diagenetic sequences, these in turn form the basis of interpretation of diagenetic events that have affected the sediments. Unravelling the sequence of diagenetic events in the Acacus sandstones is complicated by a need to be aware what diagenetic features were produced following deposition of the sands are what are inherited from elsewhere.

The subsurface sediments of the Acacus Formation in the Ghadamis Basin that have been examined are entirely clastic. The mineralogy of the sandstones has been examined by several workers (Klitzsch, 1969; Bellini and Massa, 1980; Echikh, 1985, 1998) but no data of any substance has been published.

Microscopic examination shows that the sandstones are essentially composed of detrital grains of monocrystalline and polycrystalline quartz together with minor amounts of feldspar, rock fragments, mica, heavy minerals. Detrital chlorite and phosphate grains are also present. The authigenic mineral component throughout is dominated by iron-rich chlorite (chamosite) grain coatings and cement. Pyrite and siderite are also present and together with chlorite they display the importance of iron in the depositional and diagenetic history of the formation. Some horizons contains as much as 35% iron mineral. Clay minerals other than chlorite include both kaolinite and illite. Phosphate cement is locally significant.

The following sections demonstrate that the clay minerals are both detrital and authigenic and form the

major component of the mudstones as well as a significant element of the sandstones where they are important at a number of levels. They are characteristically iron-rich and an appreciation of the origin of such iron-rich sandstone facies is critical to a full understanding of the depositional environments within the basin. An important factor in this is evaluation of the order and timing of their formation, i.e. the authigenic mineral sequence.

Chlorite, illite, and kaolinite have all been found in the Acacus Formation associated with the clean-sandstone, bioturbated sandstone, iron-rich sandstone and mudstone facies.

3.2. Clay minerals-morphologies and composition

3.2.1. Chlorite mineral morphology

In the Acacus Formation chlorite occurs as detrital-grains, grain-coating, grain rimming pore-filling and pore-lining-cements. All forms of the chlorite are pale green in color under transmitted light and show grey-yellow birefringence colors in polarized light.

3.2.2. Chlorite grains detrital

Chlorite-rich grains fall into three categories: uncoated grains, coated grains or ooids and mica replacement grains. Features of these suggests that the final event in their history was as detrital particles although the genesis of the chlorite component was authigenic.

3.2.3. Uncoated grains

These consist mainly of structureless or randomly oriented clay that is confined to a pellet-shaped rounded mass (Figure 3A-B) that shows sharply defined grain boundaries and commonly contains silt-size quartz grains. They display characteristics very similar to the glauconite grains in the sediment and are comparable in size to the associated quartz grains. The general morphology and composition of these grains is consistent with their being faecal pellets which were laterally completely chloritized, but other origins also are possible such as inorganically produced mud clasts. The sharp boundaries and equivalence in size with associated quartz grains suggests that they have undergone transport as detrital grains.

3.2.4. Coated grains

The coated chlorite grains display a nucleus consisting either of chlorite (Figures 3C-F, 4A-B) or a quartz grain (Figure 4C-D). In rare instances the nucleus consists of a cluster of two or three smaller quartz grains that are themselves partially coated (Figure 4E-F). The grains are similar to the extensively described clay ooids characteristic of iron formations (Odin and Sen Gupta, 1988). They are generally similar in size to the associated quartz grains. In some examples it is clear that the cortex is thickest where there are embayment in the nucleus (Figure 4C-D).

In others the cortex maintains a more or less even thickness (see Figure 3E) or is thicker in the long axis plane of ellipse-shaped grains (Figure 4F). In some samples, the detrital nuclei of quartz and feldspar grains are surrounded by very thin ooidal coatings and all gradations can be observed from these thin concentric coatings up to bona fide ooids where the coatings comprise 50% or more of the grain cross section. The nuclei of thinly coated grains are generally larger than those with thick cortexes. The ooidal grains make up only a small percentage of the sandstones (<10%) in which they occur. This and absence of concentric coatings on associated quartz grains of equivalent size to the ooid nuclei suggests

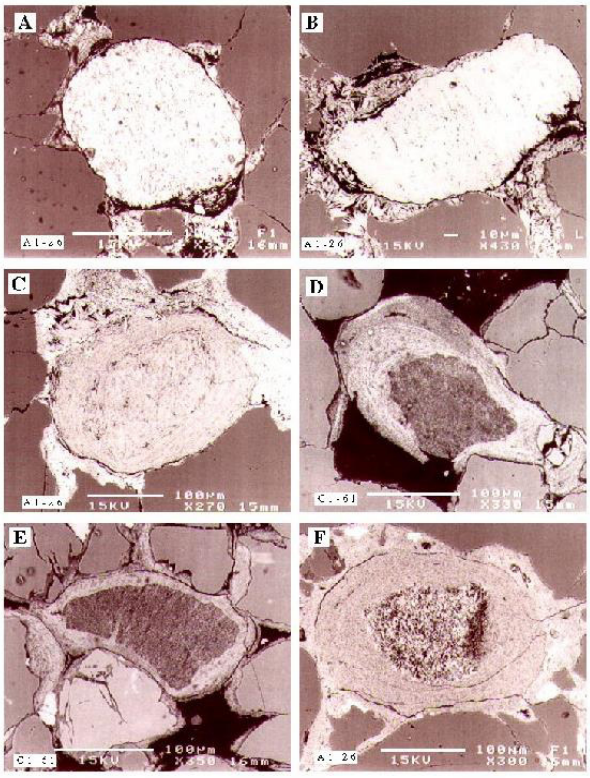

strongly that the ooids are derived in origin and have been moved from their site of formation.

Fig.3. BSEI- SEM image: A-C) Chlorite-rich pellets consisting mainly of structureless or randomly oriented clay that is confined to a rounded mass with distinct grain boundaries, (A-B), (C). D-E-F) Chlorite-rich pellets commonly are surrounded by an outer sheath of concentrically laminated clay similar to the ooids,

3.2.5. Replacement mica grains

These grains are composed of expanded mica that has been replaced by chlorite. They are commonly surrounded by an outer sheath of laminated clay coating or by pore-filling chlorite (Figure 5A-B). Microprobe analyses show that the chemical composition of the grains is similar to the surrounding coatings and pore-filling chlorite. The grains differ morphologically from expanded detrital micas associated with kaolinite in that the mica crystal is

expanded uniformly throughout, rather than being more expanded near the edges of the cleavage traces as is commonly the case with kaolinite/muscovite associations. While the origin of these grains is a replacement authigenic process the edges of the grain typically are rounded, indicating a degree of abrasion by transport after expansion (Wilson, 1992). Like the ooliths they have probably been derived from an adjacent depositional site. Chlorite is also observed replacing shell material (Figure 5D-F).

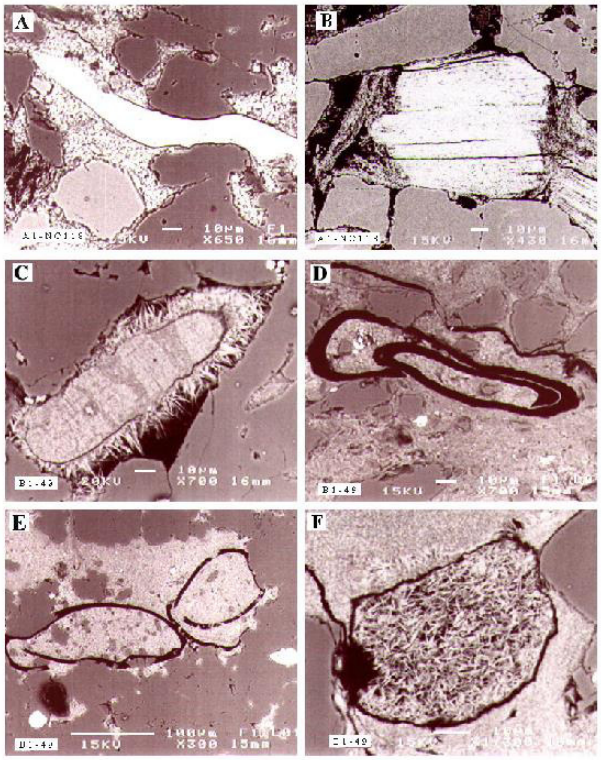

Fig. 4. BSEI-SEM image: A-B) Expanded micas replaced by chamosite. These are commonly surrounded by pore-filling chamosite or by an outer coating of chamosite. C) Late stage pore-lining chlorite growing perpendicular to the substrate and lining the pores. D-F) Authigenic chamosite infilled organism cavity surrounded by pore-filling chamosite (D-E-F)

3.3. Authigenic chlorite

3.3.1. Chlorite cement-pore-lining

This form of chlorite is very distinctive occurring as fine 'spine-like' crystals arranged perpendicular to the detrital particles to form an isopachous rim of cement about 5-10 µm thick that occasionally fills the pore spaces. Scanning electron microscopy investigation reveals that the well-developed crystal morphology (Figure 5A-F), and their particular arrangement could hardly be of detrital origin, but must have been authigenically formed by crystallization from pore solutions. The grain coating chlorite typically shows slightly curved or crenulated plates, arranged in a cellular or honeycomb pattern and is generally absent at grain contacts.

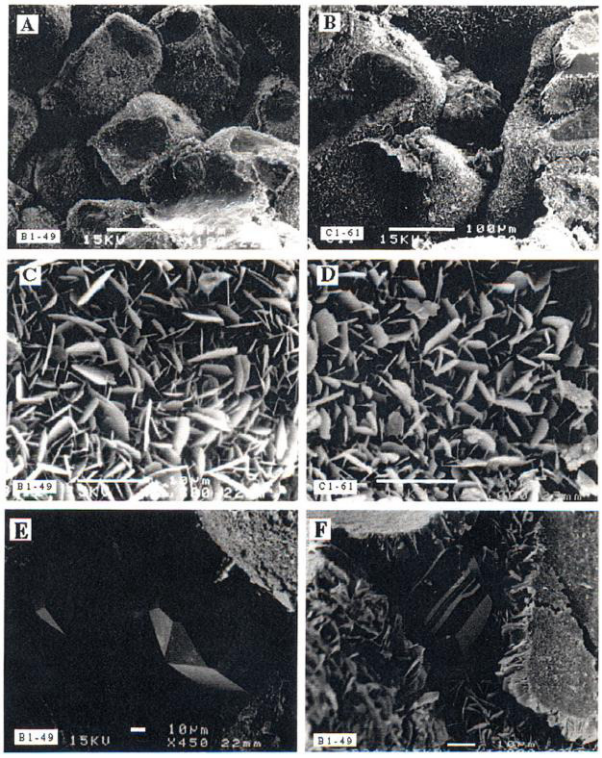

Fig. 5. SEI-SEM image: A-B) Quartz grains coated entirely by radially oriented chlorite. Note foot prints marking surfaces of contact with adjacent grains. C-D) Detailed view of authigenic chlorite rosettes composed of psedohexagonal flakes. E) Pore-lining chlorite beneath later quartz overgrowth. Several chlorite platelets are partially engulfed by the overgrowth. F) Quartz grains coated by well-developed authigenic pore-lining chlorite flakes. The quartz overgrowths can be seen enveloping plates of chlorite and are later than the pore-lining chlorite.

3.3.2. Chlorite cement-pore-lining

This form of chlorite usually consists of euhedral to subhedral crystal plates, typically 3-8µm in maximum dimension, arranged in haphazard face-to-edge card-house arrangement. Some pores are totally occluded, whereas adjacent pores may remain largely empty (Figure 6A-F). Sometimes the cement forms fan-shaped clusters of crystals (rosettes) up to 5 µm in diameter (Fig. 6B-C-D). The cement develops from outgrowth of the isopachous grain rimming cement to occlude the pore-space completely or partially (Figs. 6A). Pore-filling cement is also associated with infill of rare shell material (see Figure 5D-F). Here the shell material has subsequently been dissolved.

3.3.3. Chlorite mineralogy-XRD analysis

The chlorite is characterized by a basal reflection at 14Å and a major peak at 7Å. It can be seen that on glycolation the peaks became more intense. Slight contraction of the 14Å basal spacing to 13.6Å occurs after heating to 550oC. Other peaks disappeared except for the basal reflections, which significantly reduced in intensity. These chlorites are characterized by relatively weak (001) (14-14.05Å) and 003 (4.73Å) reflections and strong 002 (7.05Å) and 004 (3.52Å) reflections, which indicate that they are iron-rich and they are identified as chamosite.

Curtis (1983) in his study on the Tuscaloosa Sandstones, reported that the behavior characteristic of chamosite is that the 14.15Å reflection of chlorite is unaffected by glycolation but contracts to 13.6Å on heating, and the 002 reflection virtually disappears. On the basis of XRD alone, the Acacus chlorite thus has a typical chamosite structure. Whittle (1986) reported that the intensity ratio of the (001) and (002) reflections of chlorites can be used to estimate the relative importance of Fe and Mg in the octahedral sheet. Heavy cations, primarily Fe, accentuate the even-order basal reflections relative to odd-order basal reflections. Mg-rich species therefore generally have ratios of (001):(002) of the order of 5:10, whereas lower ratios suggest more Fe-rich compositions. The chlorites from the Acacus Formation have an intensity ratio of 1.0:10.0 further supporting their interpretation as chamosite.

Variations in basal spacing (001) reflect the degree of Al for Si substitution in the tetrahedral sheet, whilst the (060) reflection gives a further indication of the amount of Fe2+ in the octahedral sheet (Whittle, 1986).

Kaolinite and berthierine can create difficulties when present with chlorite. Whittle (1986) noted that in an extreme case of a sedimentary chlorite with high Fe content, it is possible that the (001) reflection may be so weak that the mineral could be misidentified as a 7Å berthierine rather than 14Å chamosite.

3.3. Chemistry of the chlorite

Use of an EDS-microprobe allows the chemistry of the chlorites, in particular the relative amounts of Fe, Mg and Al, to be determined. There are limitations in these analyses. The principal drawback is that the probe cannot separate ferrous from ferric iron. This is a problem with, for example: Recent green clay pellets or berthierine, when it has to be assumed that all the iron present is ferrous, but in reality appreciable amounts of ferric iron could be present (Odin, 1985). Another serious problem results from the fine grain size of the authigenic chlorite and its common occurrence coating detrital grains; it is often difficult to direct the beam onto the clay plates without probing the host detrital grain or other contaminants because the volume analyzed (the surface area, about 2 µm diameter, and also the depth of penetration into the sample of about 5 µm) is often greater than the dimensions of individual clay particles. Also there is possibility of minerals such as haematite or siderite becoming attached to the clay plates and adversely affecting the measured Fe:Mg:Al ratio (Curtis et al., 1984).

Normal uncovered petrographic thin section coated by carbon were used for SEM examination of the studied samples. Average of EDS-microprobe results for the chlorite are recalculated on the basis of 20 oxygen and 16 hydroxyls. In all cases, oxide totals are less than the expected 85-88% for chlorite with an O10(OH)8 unit cell, a common problem for chlorite and mixed-layer chlorite minerals. Hillier (1994) attributed low oxide totals obtained by microprobe analyses to microporosity between chlorite grains.

The chemical data determined by microprobe analyses showed that all authigenic pore-lining chlorite and pore-filling chlorites have a relatively restricted composition range (Table. 1).

Substitution of Al for Si in the tetrahedral sheet occurred to only a moderate degree, with Al occupying 2.67 to 3.49, 2.80 to 3.38 and 2.92 to 4.64 in wells A1-26, C1-61, and B1-49, respectively, of the 8 tetrahedral sheet (full-cell basis). Fe and Al where important octahedral cations together with relatively small amounts of Mg.

All ratios of Fe/(Fe+Mg) were relatively high at 0.85-0.89, 0.78-0.91, and 0.86-0.90 in B1-49, A1-26 and C1-61, respectively. The majority of the chlorites would be described as Al-rich, Mg-chamosite according to AIPEA nomenclature (Bailey, 1980).

Table. 1. Chlorite composition estimated from EDS-microprobe analyses of the Acacus Formation in the studied samples.

Well	Structural formulae	Fe/(Fe+Mg)
A1-26	$(Fe_{7.45}Al_{3.07}Mg_{1.06})[(Si_{5.50}Al_{2.50})O_{20}](OH)_{16}$	0.91
C1-61	$(Fe_{7.43}Al_{3.02}Mg_{1.55})[(Si_{5.74}Al_{2.26})O_{20}](OH)_{16}$	0.91
B1-49	$(Fe_{6.24}Al_{3.67}Mg_{1.07})[(Si_{5.85}Al_{2.15})O_{20}](OH)_{16}$	0.89
A1-NC40B	$(Fe_{6.99}Al_{3.19}Mg_{1.10})[(Si_{5.82}Al_{2.18})O_{20}](OH)_{16}$	0.89
A1-NC118	$(Fe_{6.59}Al_{3.38}Mg_{1.30})[(Si_{5.75}Al_{2.25})O_{20}](OH)_{16}$	0.90

All collected data were processed through to standard weight percent ratio and molecular formulae. The data for each well were then plotted on triangular diagrams. On these the various elements were plotted against each other to give scatter plots. Aluminium and magnesium are plotted against iron shows a distinct trend developed towards the iron corner and the Al: Mg ratio appears to be very constant.

The compositional range of the common trioctahedral chlorite can be usefully depicted in the following paragraph.

Probe data for the Acacus chlorite are summarized on a Fe-Mg-Al triangular plot in Figure 8. The diagram also shows fields of the known compositional range of detrital metamorphic chlorite, diagenetic chlorite and berthierine, taken from Velde (1985). It can be seen that most of the chlorite falls within the field of metamorphic chlorite. The Acacus chlorite clearly plot as iron-rich chlorite (chamosite).

Results are plotted on a Fe-Mg-Al and Si-Fe-Al triangular plots (in Mol% element) in Figure 9a-b, taken from Curtis et al., (1985), Jahren and Aagaard (1989) respectively. It can be seen that most of the studied chlorite fall within the field of iron pole,

indicating the Acacus chlorite clearly plot as iron-rich chlorite (chamosite).

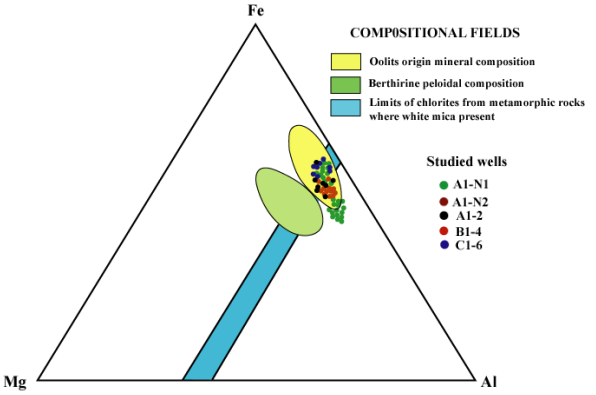

Fig. 8. Summary diagram of EDS-microprobe data presented on a total Fe-Mg-Al plot for the chlorite from the Acacus Formation, fields taken from Velde, 1985.

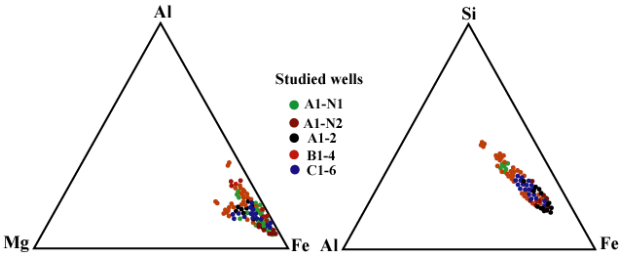

Fig. 9. A, B) EDS-microprobe analyses of chlorite, plotted on the major-element diagram (in Mol%). Compositional plot taken from (A) Curtis et al. (1985); (B) Jahren & Aagaard (1989).

A different type of plot is shown in Figure10, after Hayes (1970) and Curtis et al., (1985), where values of tetrahedral Al (calculated as 8 minus Si) are plotted against the ratio of octahedral Fe/(Fe+Mg). In this case a slight chemical difference between the grain coating and pore-filling chlorites is apparent, with the former showing a tendency towards lower Fe/(Fe+Mg) ratios. Anomalously high Si contents are indicated by some low values of tetrahedral Al. Average values of the octahedral totals for the Acacus chlorites approximate to 11.00, considerably less than the theoretical total of 12.00. Octahedral Al exceeds tetrahedral Al in many sedimentary chlorites and will account for the departure from an ideal formula (Whittle, 1986).

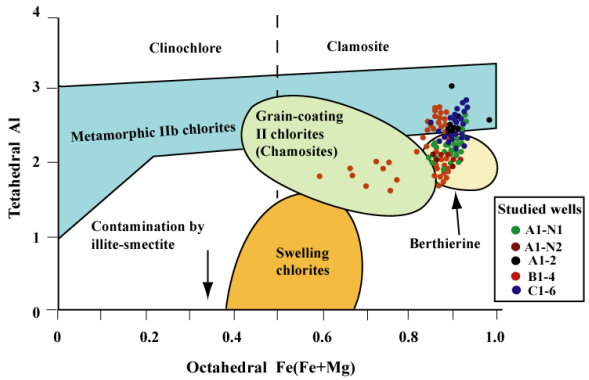

Fig. 10. Plot of tetrahedral Al against octahedral Fe/(Fe+Mg) for the Acacus chlorite. Compositional fields for metamorphic chlorite, chamosite and swelling chlorite are taken from Hayes (1970) and Curtis et al. (1985).

3.4. Inherited features

Grains within a sand may contain diagenetic features that were formed in the source area prior to transportation of the grains and thus have nothing to do with the diagenetic processes that occur following deposition at their new site. The grains thus display features that are inherited from an earlier phase of diagenesis at an earlier adjacent site.

It was noted that some chamosite grains within the sands are coated with chamosite while most others are not and it was proposed that these are detrital particles. The coatings range from:

Full concentric zoned cortex giving typical ooids (Fig. 11A). The cortexes of these may be chamosite or iron oxide.

Partial coatings-possibly due to erosion of part of the cortex (Figures 11B, C, and 15C)

Partial coatings also occur in embayment in grains. Wilson (1992) describes similar clay coating texture at the result of passage of the grains through the gut of marine organisms (Figure 11D, E).

A thin surface coating (Figure 11F). This layer may completely coat a grain or only part of it. The chamosite crystals as in the ooidal cortex layers are arranged tangential to the host grain.

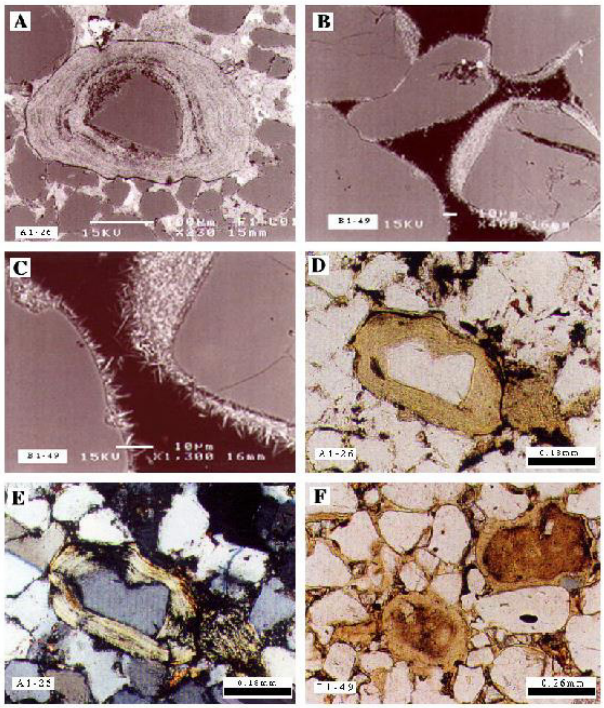

Fig. 11. BSEI-SEM image and microphotographs: A) Quartz grain surrounded by a concentric zoned chamosite cortex giving typical ooids. B) Partial coatings of quartz grain by chamosite possibly due to erosion of part of the cortex of the chamosite. C) Enlarged view. D-E) Ooliths in which grain coating infill embayment's in grains. Note how the coating is thickest over the embayed part of the grain (D) PPL, (E) XN. F) Quartz grains show thin surface coatings. The chamosite crystals as in the ooidal cortex layers are arranged tangential to the host grain. Note two inherited ooids and compaction of cortex.

The parent grains are dominantly quartz with some feldspar, and rare detrital siderite and haematite,

rutile. Other grains are composite and comprised of several grains cemented by chamosite, the whole being contained in a quartz overgrowth which in turn has a thin chamosite coating (Fig. 12A).

It is clear that the coated grains, both single and composite, have been derived from an adjacent location where oolitic iron-rich sediments were being generated and they, together with non-coated grains, make up the detrital component of the sands. This detrital component has then undergone diagenesis on burial with development of a suite of diagenetic features.

3.5. Diagenetic features-chronological relationships

As noted above there is a range of diagenetic minerals in the sandstones. Other diagenetic features include grain dissolution and compaction. The most obvious diagenetic minerals phases are chamosite, siderite and, locally, haematite cements and these serve as a good framework within which to evaluate the order of events.

3.5.1. Chamosite

The detrital component, i.e. grains with various forms of inherited clay textures together with non-coated grains, is first cemented by a pore-lining chamosite cement which shows very well developed crystal growth oriented edge-on to the host grain (Fig. 12B). This pore lining cement is succeeded in some instances by more chamosite of similar crystal habit but randomly oriented which serves as a pore-filling (Fig.12C). In some samples the pore-lining chlorite appears to develop from a grain coating layer (see Fig.12B) suggesting that the framework gains were mobile in the initial stages of chlorite formation.

3.5.2. Siderite

The pore-lining and pore-filling chlorite are succeeded by siderite which: (1) replaces the chamosite. In some instances the siderite appears to nucleate around organ ic matter giving the rock a spotted appearance (Fig.12D). Commonly the replaced mineral can be seen as a ghost form within the siderite (Fig.12E). (2) Fills pore space as a poikilotopic cement, often replacing some of the pore-lining chamosite (Fig. 12F, 13E). (3) Forms idiomorphic crystals within dissolution pore space (Fig. 13A).

3.5.3. Iron oxide

This is common in the reddened iron-rich beds (Fig. 16). It replaces chamosite and quartz forming a poikilotopic cement (Fig. 13B) and it is clear that it commonly replaces siderite grains (Fig. 13C) and that the textural similarity results from this pseudomorphic relationship. Replacement of the margins of chamosite ooliths and glauconite grains is common.

3.5.4. Quartz overgrowth

The common diagenetic sequence of chamosite cement followed by siderite, with in some instances subsequent replacement by iron oxide, is complicated

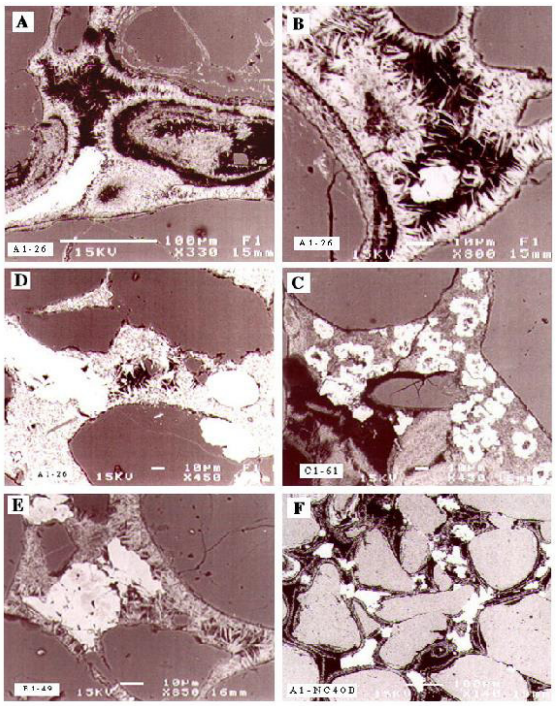

Fig. 12. BSEI-SEM image: A) Pore-lining chamosite crystals growing perpendicular to the substrate grains and lining the pores. Concentric pore space between the lining chlorite and the host grain may be due to dissolution of an earlier cement. B) Pore-lining chamosite showing very well developed crystal growth oriented edge-on to the host grain. (A-B) C) Pore-lining chamosite which has developed pore-filling cement. Note authigenic siderite that postdates chlorite. D) Authigenic siderite replacing pore-filling chamosite. E) Pore-lining and filling chamosite replaced by siderite. Note ghosts of chamosite within siderite. F) Poikilotopic siderite filling pore space. Note dissolution rims between grains and pore lining cement.

by the presence of quartz overgrowth and kaolinite together with grain dissolution.

It can be seen in Figure 13D that where grain coating on an inherited coated grain was incomplete syntaxial quartz overgrowth has taken place on the parts of the quartz grain surface that was exposed. A further example is seen in figure 13E. The pore-lining chamosite is later than this quartz overgrowth. The pore-lining chamosite in turn, however, is succeeded by a later quartz overgrowth which locally engulfs the edge-on grains (Figs. 13F and 14A). It is proposed therefore that quartz overgrowth developed in at least two stages - Q1 and Q2. Quartz overgrowth Q2 (and hence Q1) is, however, clearly earlier than the poikilotopic siderite (Fig.14B) and also granular siderite which can be seen to replace it (Fig. 14C).

3.5.5. Kaolinite

Well-developed kaolinite occupies intergranular pore space where it is clearly post-dates the pore-lining chamosite (Figs. 14D and 14E). It also occurs in grain dissolution cavities pre-poikilotopic siderite (Fig. 14F and Figure 15A). It can be seen in Figure 15B and Figure 11D that it is earlier than siderite that replaced pore-filling chamosite.

3.5.6. Grain dissolution

Remains of K-feldspar in grain dissolution cavities suggests that most of the grain dissolution porosity in the sandstones is due to solution of this mineral (Figure 15C). The presence of kaolinite in many such cavities tends to support this view. It is also however, likely that in pores where total dissolution has taken place, the grains that were removed may have been plagioclase feldspars. More unusual is the partial dissolution of grains leaving a euhedral grain network of ilmenite/rutile. This network is similar to the exsolution patterns found in ilmenite/titanomagnetite grains (Amini, 1997).

3.5.7. The timing of grain dissolution

Grain dissolution is certainly pre-siderite as shown by idiomorphic authigenic crystals of siderite in pore cavities (Figures. 13A and 15E) and earlier than kaolinite which infill many of the dissolution pores. It has already been noted that the kaolinite is earlier than siderite (Figure 15B) where seen in intergranular pore space. The relationship to quartz overgrowth is not entirely clear. Figure 15F shows an inherited grain with a well-developed thin ooidal chamosite coating on a feldspar nucleus. The feldspar is partly dissolved. A quartz overgrowth hosted on an adjacent quartz grain stops at what would appear to be the original boundary of the dissolved feldspar grain. It appears to replace its original inherited chamosite coat. This quartz displays a similar relationships to Q1 described above and it would appear that dissolution was post Q1 otherwise the overgrowth might have continued into the pore space. In contrast, siderite grows into the dissolution space.

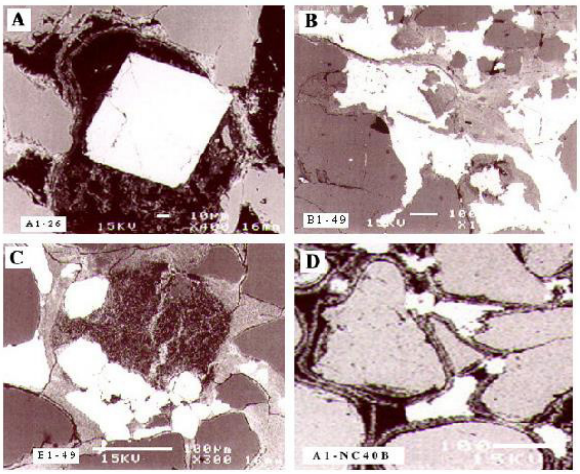

Fig. 13. BSEI-SEI-SEM image: A) Siderite forming idiomorphic crystals within dissolution pore space of unstable detrital grains. B) Iron oxide forming a poikilotopic cement and replacing quartz and pore-filling chamosite. C) Iron oxide replacing margins of quartz and glauconite grains. Here it clearly pseudomorphs earlier siderite crystals. D) Quartz overgrowth on parts of quartz grain surface not coated by chlorite.

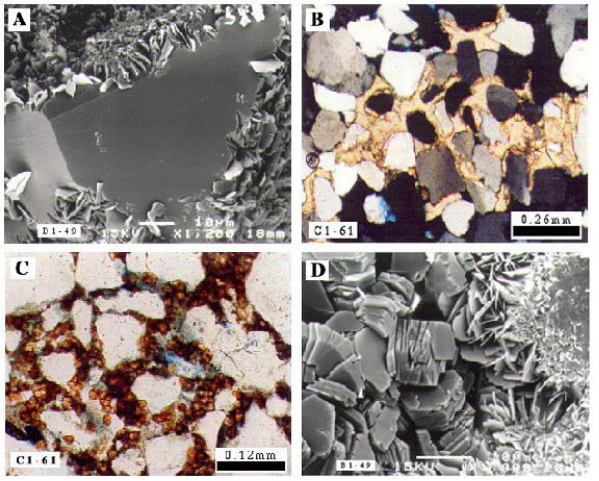

Fig. 14. BSEI-SEI-SEM image and microphotographs: A) Late stage of quartz overgrowth engulfs the edge-on quartz grain and enveloping plates of chamosite. B) Quartz overgrowth is clearly earlier than poikilotopic siderite. C) Granular siderite replace quartz overgrowth. D) Well-developed kaolinite postdates the pore-lining chamosite.

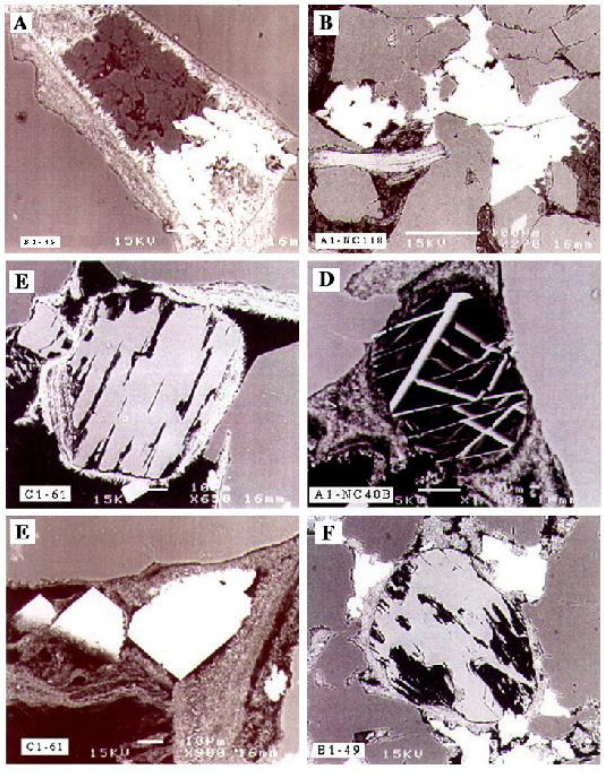

Fig. 15. BSEI-SEM image: A) Kaolinite occurs in grain dissolution cavities post pore-lining chamosite and earlier than siderite. B) Kaolinite is earlier than siderite that replacing pore-filling chamosite. C) Grain dissolution of K feldspar. D) Euhedral grain network of ilmenite/rutile is due to grain dissolution. E) Idiomorphic authigenic crystals of siderite in pore cavities. F) Inherited grain with a well-developed thin ooidal chamosite coating on a feldspar nucleus.

In Figure 16A a quartz overgrowth that appears to be pre pore-lining chamosite stops at what would appear to have been the original grain boundary,

indicated by extent of kaolinite infill. This suggests that quartz overgrowth was pre-dissolution and pre pore-lining chamosite as described above. However, an alternative explanation is that dissolution of the 'feldspar' was post pore-lining chamosite. This chamosite would have been absent at the original grain contact between quartz and feldspar. Dissolution of the feldspar would have exposed the quartz at the grain contact allowing nucleation of a quartz overgrowth on the quartz grain which was protected elsewhere by the pore-lining chamosite. It is proposed therefore that dissolution was post development of pore-lining chamosite and that Q2 was post dissolution and pre-, or coeval with, kaolinite precipitation.

3.5.8. Pyrite

Framboidal pyrite is seen to postdate detrital illite (Figure 16B) and it appears to be closely associated with organic matter. Its relationship to authigenic illite has not been seen. It appears to be later than chlorite. In figure 16C pyrite framboids replace chamosite.

In contrast, in figure 16D framboids cluster around the margin of a grain dissolution pore are enclosed in pore-filling kaolinite. Its relationship with quartz overgrowths is ambiguous - figure 16E suggest that it is earlier but in figure 16C is appear to be later. The age relationship with siderite is not seen as siderite appears to be absent where pyrite is present.

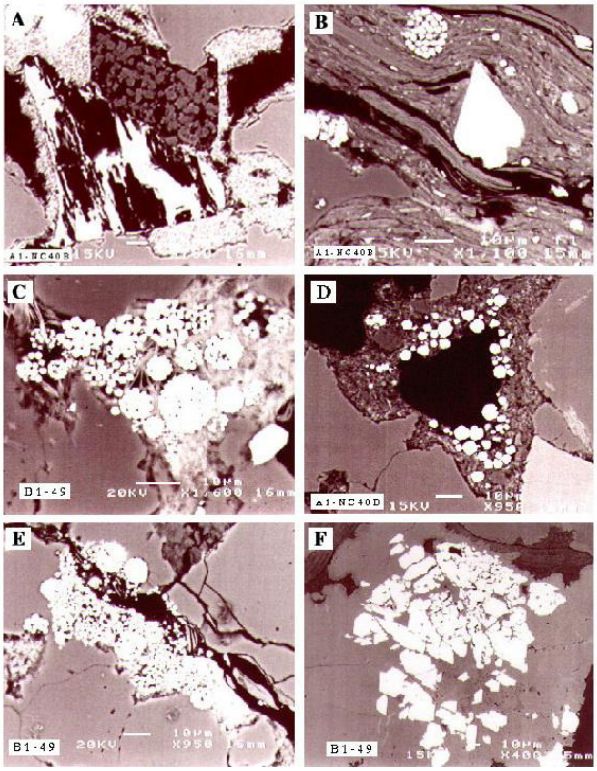

Fig. 16. BSEI-SEM image: A) Quartz overgrowth post dissolution of K feldspar and pre or coeval with kaolinite cement. B) Framboidal pyrite postdate detrital illite. C) Framboidal pyrite replaces chamosite. D) Framboids cluster pyrite around the margin of a grain dissolution pore. E) Early stage of pyrite precipitation. F) Euhedral pyrite replaces both overgrowths and quartz-grains.

3.5.9. Apatite

Apatite mineralization displays a similar relationship to chamosite and quartz overgrowth to that of siderite. It occurs as: Replacement of pore filling chamosite (Figure 17A) with stubby idiomorphic crystals that also grow in pore space. Figure 17B shows such crystals replacing pore filling chamosite in a shell interior. The rest of the shell fill is a geopetal-like fill with fine chamosite and quartz 'mud' and a clear coarse quartz cavity fill.

Poikilotopic pore-filling cement (Figure 17C).

Grain coating (Figure 17D)

Figure 17C shows that the poikilotopic cement is post quartz overgrowth. Figure 17B, summarizes the overall relationships well. Here poikilotopic apatite fills a grain dissolution cavity. The dissolution that formed the pore was post pore-lining chamosite. Quartz overgrowth was post dissolution and the apatite cement encloses all the earlier phases.

Apatite overgrowth is rare but is seen as a thin layer coating a phosphate fragment (Figure 17D). It can be seen that this is pre chamosite pore fill. An unusual overgrowth occurrence is shown in Figure 17F. Here a feldspar grain with a partial coating of chamosite is overgrown by a thin layer of apatite. The layer is absent at the feldspar/quartz grain contact and thins where the two come close together. The layer is succeeded by pore-lining chamosite which appears to be entrapped in quartz overgrowth. This apatite is thus earlier than any other apatite recorded. No other grains in this sample displayed the type of overgrowth.

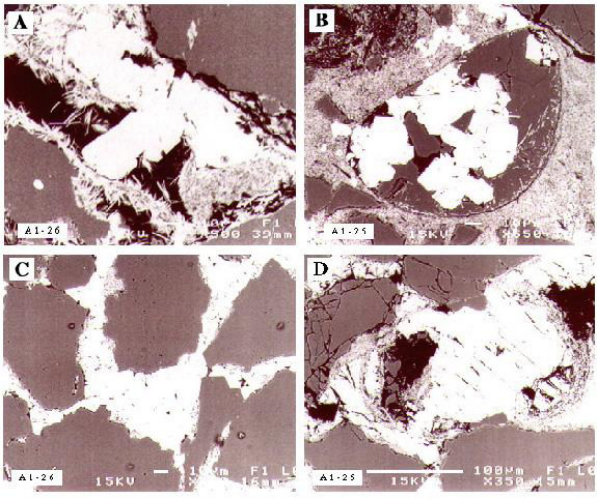

Fig. 17. BSEI-SEM image: A) Apatite replacing pore filling chamosite, also grow in pore space with stubby idiomorphic crystals. B) Apatite replacing pore-filling chamosite and a shell interior. C) Poikilotopic cement is post quartz overgrowth. D) Apatite overgrowth is rare but is seen as a thin layer coating a phosphate fragment.

3.5.9. Illite

Relationships between illite and chamosite have not been observed in the sections studied other than the presence of an illite pore-fill in which details were not resolved. Illite appears to be the clay mineral present when chamosite is absent although XRD suggests that

they do occur together. Illite-rich sandstones contain the greatest concentrations of pyrite and illite is much more common in the mudstones that other clay minerals.

3.6. Physical diagenetic features

3.6.1. Compaction

Compaction features are rare. Preservation of delicate remnant pore-lining cement zones around grain dissolution pore space implies that dissolution was post major compaction. Figure 18 shows a fractured K-feldspar where fracturing may have been post pore-lining chamosite although the concavo-convex contact between feldspar and quartz is clearly pre pore-lining chamosite.

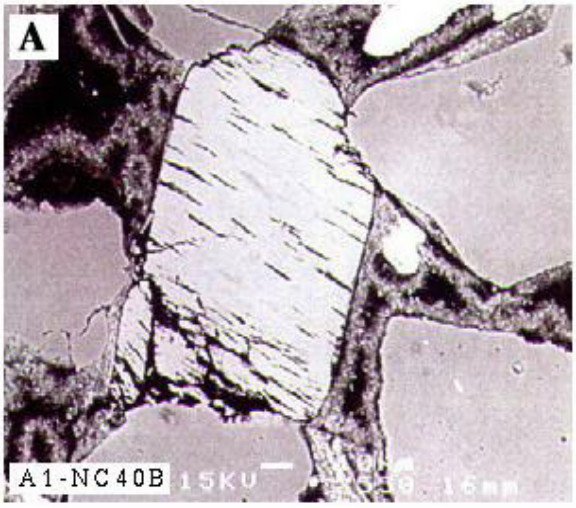

Fig. 18. BSEI-SEM image: Fractured K feldspar which is probably post pore-lining chamosite.

3.6.2. Porosity

In addition to grain dissolution porosity noted above there is intergranular porosity some of which may be primary but most of which is more likely to be secondary. One feature of this secondary porosity is a thin pore zone between pore-lining chamosite and the host grain seen in many samples (Figures. 12A-B, 15D, and 18).

3.7. Origin of the diagenetic mineral sequences in the Acacus formation

The chronological relationships described above suggest three sequences which are closely related:

- Chamosite ⟶ Siderite
- Chamosite ⟶ Apatite
- Chamosite ⟶ Pyrite

The first two display in some cases a final in which the Fe(II) minerals are oxidized and replaced by Goethite and Haematite.

3.7.1. Chamosite-origin

A number of possibilities, not mutually exclusive, were listed as to the origin of chamosite:

(1) Alteration of precursor kaolinite.
(2) Transformation of a swelling chlorite (corrensite).
(3) Transformation of interstratified serpentine chlorite.
(4) Transformation of berthierine.

In addition, the dissolution of K feldspar is a source for late chloritic diagenetic clays. It is generally agreed that perhaps the most common precursor is berthierine and that this transforms to chamosite on burial. It is proposed that the initial iron silicate formed in the Acacus Formation was berthierine. The secondary nature of the Acacus chamosite is supported by the data shown in figure 10 which indicates that it is 'metamorphic'

3.7.2. Chamosite-siderite

The close occurrence of iron silicate and siderite cements in iron-rich sediments has been widely reported and the chemical conditions governing their precipitation and relationships have been widely discussed. The work of Taylor and Curtis (1995) and MacQuaker et al., (1996) is particularly relevant to the present situation.

Taylor and Curtis (1995) show that precipitation of berthierine takes place as a result of "destabilization of detrital clay minerals" during early stages of suboxic diagenesis. This is related to high Fe^{2+} pore water activities resulting from iron reduction which they point out produces "four times as much Fe(II) as HCO_3^-. Continuing suboxic diagenesis shows a decrease in iron activities and a corresponding increase in carbonate activity (Curtis and Spears 1968). When high CO_2 pore water activity is attained siderite precipitation takes over from berthierine.

3.7.3. Chlorite-siderite-iron oxide

It was shown in section that the iron oxide cements displays a closely similar composition to siderite in terms of its content of iron, magnesium and manganese content. This strongly indicates that the much of the iron oxide formed by oxidation of the siderite and original berthierine.

Oxidation of berthierine oolites cortexes and glauconite grain margins was most likely to have occurred by redox recycling due to reworking of the sediments at the site of oolite formation (Taylor and Curtis, 1995) from where they were transported into the present site of deposition as detrital grains. It can be seen that the iron oxides have a lower Mg content that the siderite suggesting that Mg was leached during the oxidation process.

3.7.4. Chlorite-apatite-goethite-apatite

MacQuaker et al., (1998) show that phosphate cements develop from phosphorous released by dissolution of phosphatic skeletal fragments and organic matter. They note from the work of Nathan and Sass (1981) that as apatite precipitation is favored over carbonate precipitation at low pH values, the

presence of apatite cements suggest that the pore waters were acidic at the time of formation.

In the present case where the apatite precipitation follows the berthierine/chamosite in close association, forming grain coatings, the establishment of oxic conditions necessary for generation of acids at the oxic/suboxic/sulphidic zone boundary would almost certainly also have lead to oxidation of the berthierine. Regeneration of berthierine in a subsequent reducing environment would be difficult. Acid pore waters could however, be produced at the suboxic-sulphate reduction zone boundary by migrated methane gas (MacQuaker, pers. comm). Precipitation of chlorite/chamosite onto the apatite coating cement (Fig.17A), suggests in fact that reducing conditions prevailed throughout precipitation of such coatings but that iron availability varied. Interlamination of apatite and berthierine in ooid cortexes was described by Karasek (1981) and he proposed that they are diagenetic increments on micro-nodules.

It would appear therefore that apatite can co-exist in alternation with both reduced and oxidized iron minerals. In each case the alternation is due to variation in diagenetic conditions coupled with restriction of sediment supply.

The pore filling apatite, most clearly developed as thin cemented layers in samples from Well A1-26, is clearly associated with iron oxides and is later than both haematite cement and haematite coated ooids. It would appear that the oxides such as haematite and magnetite were more or less stable in the reducing conditions necessary for apatite formation. Harder (1980) notes that this is due to their low solubility and reactivity and states that even under conditions favorable for precipitation of berthierine and siderite that haematite and magnetite may also be present.

3.7.5. Chamosite-pyrite

This relationship arises from a change from conditions in the suboxic zone with precipitation of chlorite to conditions of the sulphidic zone where reduction of dissolved sulphate leads to production of hydrogen sulphide. Combination of reduced iron with HS- forms the iron pyrite. The relationships seen would appear to have resulted from gradual burial of the sediment and its progression from the suboxic into the sulphate reduction diagenetic zones.

The association of pyrite with the finer sediments such as the clay and silt-rich mudstones is significant. These deposits were probably deeper and possibly more stagnant water and likely to have had reduced oxygen in the pore waters near the sediment water interface. The sub-oxic and sulphate reduction zones may therefore have been present near to or at the sediment water interface. In such conditions the preferred iron mineral precipitate at shallow depths within the sediment would be pyrite.

3.7.6. Feldspar grain dissolution

It has been shown above that feldspar grain dissolution, quartz overgrowth Q2 and kaolinite precipitation all pre-date siderite precipitation. They also predate apatite precipitation. One example of authigenic siderite shows crystals that appear to pre-date quartz overgrowth but the planar grain contacts suggests that there may have been pressure dissolution of the quartz overgrowth.

3.7.7. Kaolinite

The grain dissolution pore-filling kaolinite can be considered as a by-product of the feldspar dissolution. Intergranular pore-filling kaolinite may have a similar origin and been redistributed by pore waters, although some may have formed at later stages.

3.7.8. Quartz overgrowth

The source of silica for quartz overgrowth associated with grain dissolution cavities is most probably related to feldspar dissolution and kaolinite formation. Extensive overgrowth that is present in some of the sandstones is more likely to be due to the other sources noted above as it is unlikely that enough feldspar was available to supply all the quartz. Underlying shale of the Tannezuft Formation as well as interbedded shale's would be a likely source for such silica.

The early quartz overgrowth Q1 pre-dates development of pore-lining chlorite and dissolution, events that have been attributed to reactions in the suboxic and sulphate reduction zones. It is therefore very early diagenetic, almost certainly pre-compaction, and may have occurred in the oxic zone. Absence of associated kaolinite and feldspar suggest that the source of silica was from organic material.

3.8. Pore-lining-Porte Walls GAP

It is the pore-lining layers that have contracted. The gap was initially filled with a cement which has since been dissolved.

The first case demands that the original coatings and pore fill were not berthierine but some other mineral. The proposal by Curtis (1985) that chamosite could form from smectite through an intermediate swelling chlorite is interesting in that this could explain possible contraction on formation of the berthierine/chamosite. The presence of a carbonate rim cement, since removed, would, however, seem more likely. Preservation of such a delicate texture implies that its formation is post compaction. The phenomenon needs much further study.

4. Conclusion

The diagenetic sequences are summarized in the following.

- The sequence for chlorite-apatite is similar to that for chlorite-siderite except that apatite forms instead of the siderite due to removal of

Fe^{2+} by restriction of iron detrital fragment input coupled with oxidation.

- In the chamosite-pyrite trend pyrite was precipitated from sulphide released by sulphate reduction combining with Fe^{2+} as the sediment was buried and passed into the sulphate reduction zone.
- It can be seen that the sequences and the mineral types are facies related with muddy sands and shale's being richer in pyrite with little or no siderite.
- In addition to the three sequences shown, a fourth sequence is seen in the rare levels of clean quartz sandstones. Here there is well-developed quartz overgrowth, related to intergranular and grain-dissolution porosity and the only cement is siderite. This replaces the overgrowth and partially occludes porosity.
- The various sequences form an important part of interpreting observed facies change and the setting up of a depositional model.

References

Amini, A., 1997. Provenance and Depositional Environment of the Upper Red Formation, Central Zone, Iran (Unpublished Ph.D. Thesis). Manchester University.

Bailey, S. W., 1980. Structures of the layer silicates, In: Brindley, G. W., and Brown, G., (eds.) Crystal structures of clay minerals and their X-ray identification, Mineralogical Society, London, Monograph, 5, 1-123.

Bellini, E., and Massa, D., 1980. A stratigraphic contribution to the Paleozoic of the Southern basins of Libya. In: Salem M. J. and M. T., Busrewil (eds.) 2nd Symp. Geology of Libya. Univ. Libya, Fac. Sci., Tripoli, 1, 3-27.

Bishop, W. F., 1975. Geology of Tunisia and adjacent parts of Algeria and Libya, Am. Ass. Petrol. Geol, Bull, 59 (3), 413-450.

Brown, G., and Brindley, G. W., 1980. X-ray diffraction procedures for clay mineral identification, In: Brinley, G. W., and Brown, G., (eds.) Crystal structures of clay minerals and their X-ray identification, Miner. Soc. London, Monograph, 5, 305-359.

Clifford, A. C., 1986. African oil-past, present, and future, Am. Ass. Petrol. Geol., Mem., 40, 339-372.

Curtis, C. D., 1983. Geochemistry of porosity enhancement and reduction in clastic sediments. In: Brooks, J. (ed.) Petroleum geochemistry and exploration of Europe, Blackwell Scientific Publ., 113-125.

Curtis, C. D., 1985. Clay mineral precipitation and transformation during burial diagenesis, Phil. Trans. R. Soc. London, A315, 91-105.

Curtis, C. D., and Coleman, M. L., 1986. Controls on the precipitation of early diagenetic calcite, dolomite, and siderite concretions in complex depositional sequences, in Gautier, D. L. (ed.), Roles of organic matter in sediment diagenesis, Soc Econ. Paleont. Miner. Spec. Publ., 38, 23-33.

Curtis, C. D., and Spears, D. A., 1968. The formation of sedimentary iron minerals, Econ. Geol., 63, 257-270.

Curtis, C. D., Huges, C. R., Whiteman, J. A., and Whittle, C. K., 1985. Compositional variation within some sedimentary chlorites and some comments on their origin. Miner. Mag., 49, 375-386.

Curtis, C. D., Ireland, B. J., Whitman, J. A, Mulvaney, R., and Whittle, C. K., 1984. Authigenic chlorites: problems with chemical analysis and structural formula calculation, Clay Miner., 19, 471-481.

Deer, W. A., Howie, R. A., and Zussman, J., 1992. An introduction to the rock forming minerals, Longman, London. 720pp.

Echikh, K., 1985. Sedimentological conditions of deposition and petroleum evaluation of Acacus-Tanezzuft reservoirs, Internal Report, National Oil Corporation of Libya (NOC), Tripoli, Libya.

Echikh, K., 1998. Geology and hydrocarbon occurrences in the Ghadames Basin, Algeria, Tunisia, Libya. In: Macgregor, D. S., Moody, R. T. J., and Clark-Lowes, D. D., (eds.) Petrol. Geol. North Africa, Geol. Soc. London, Spec. Publ., 132, 1090-129.

Harder, H., 1980. Synthesis of glauconite at surface temperatures. Clay and Clay Miner., 28, 217-222.

Hayes, J. B., 1970. Polytypism of vhlorite in sedimentary rocks, Clays Clay Miner., 18, 285-306.

Hea, J. P., 1971. Petrography of the Paleozoic-Mesozoic sandstones of the southern Sirte Basin, Libya, In: Gray, C. (ed.) 1st. Symposium. Geol. Libya, Univ. Libya Fac. Sci., Libya, 107-125.

Hillier, S., 1994. Pore-lining chlorites in siliciclastic reservoir sandstones: Electron microscope, SEM, and XRD data, and implications for their origin, Clay Miner., 29, 665-679.

Jahren, J. S., and Aagaard, P., 1989. Compositional variation in diagenetic chlorites and illites, and their relationships with formation water chemistry, Clay Miner., 24, 157-170.

Karasek, R. M., 1981. Structural and straitgraphic analysis of the Paleozoic Murzuk and Ghadamis Basins, western Libya, (Unpublished. PhD Thesis), University of South Carolina, Columbia, SC.

Klitzsch, E., 1969. Stratigraphic section from the type areas of Silurian and Devonian strata at western Murzuk Basin, Libya, In: Kanes, W. H. (ed.) Geology, archaeology and prehistory of the southwestern Fezzan, Libya, Petrol. Explor. Soc. Libya, 11th Ann. Field Conf., 83-90.

MacQuaker, J. H. S., Gawthorpe, R. L., Taylor, K. G., and Oates, M. J., 1998. Heterogeneity, stacking patterns and sequence stratigraphic interpretation in distal mudstone successions: Examples from the Kimmeridge Clay Formation, U.K., In: Schieber, J., Zimmerle, W., and P. S. Sethi (eds.), Shales and mudstones, 1, Basin studies, sedimentology, and paleontology, E. Schweizerbart'sche Verlagsbuchhandlung (Nagele u. Obermiller), Stuttgart, 163-186.

MacQuaker, J. H. S., Taylor, K. G., Young, T. P., and Curtis, C. D., 1996. Sedimentological and geochemical controls on ooidal ironstone and bone-bed formation and some comments on their sequence-stratigraphical significance, in: Hesselbo, S. P. and Parkinson, D. N. (eds.) Sequence stratigraphy in British Geology, Geol. Soc. London, Spec. Publ., 103, 97-107.

Nathan, Y., and Sass, E., 1981. Stability relations of apatites and calcium carbonates. Chemical Geology, 34, 103-111.

Elsevier, Amsterdam and New York.

Odin, G. S., 1985. La "Verdine" facies granulaire vert marin et cotier distinct de la glauconite: distribution actuelle et composition, compte Rendus de L'Academie des Sciences de Paris, 301, 2, 105-118.

Odin, G. S., and Sen Gupta, B. K., 1988. Geological significance of the verdine facies. 159-204. In: Odin, G. S., (ed.) Green marine clays, Elsevier, Amsterdam and New York.

Shah S. H. A., Mansouri, A. and Al-Ghoul, M. (1993) Paleozoic sandstone reservoirs of the Hamada Basin, NW Libya: effects of sedimentary processes on porosity, Jour. Petrol. Geol., 16, 3, 345-352.

Taylor, G. K., and Curtis, C. D., 1995. Stability and facies association of early diagenetic iron mineral assemblages: an example from a Jurassic ironstone-mudstone succession, U.K., Jour. Sediment. Research, A65, 2, 358-368.

Velde, B., 1985. Clay minerals: A physico-chemical explanation of their occurrence, Elsevier, Amsterdam, 427pp.

Whittle, C. K., 1986. Comparison of sedimentary chlorite compositions by X-ray diffraction and analytical TEM, Clay Miner., 21, 937-947.

Wilson, M. D., 1992. Inherited grain-rimming clays in sandstones from eolian and shelf environments: their origin and control on reservoir properties, In: Houseknecht, D. W., and Pittman, E. D., (eds.) Origin, diagenesis, and petrophysics of clay minerals in sandstones, Soc. Econ. Paleont. Miner. Spec. Publ., 47, 209-225.